

iREVIEW

IMAGING FOR BEST OUTCOMES IN STRUCTURAL HEART INTERVENTIONS SPECIAL ISSUE

Imaging for Patient's Selection and Guidance of LAA and ASD Percutaneous and Surgical Closure



Francesco F. Faletra, MD,^a Muhamed Saric, MD,^b Jacqueline Saw, MD,^c Mathieu Lempereur, MD,^d Thoesten Hanke, MD,^e Mani A. Vannan, MD^f

ABSTRACT

This review comprises 2 main subjects: the percutaneous and surgical closure of the left atrial appendage (LAA) and atrial septal defect (ASD). The aim of the authors was to provide a detailed description of: 1) anatomy of LAA, normal interatrial septum, and the various types of ASD as revealed by noninvasive imaging techniques; 2) preprocedure planning of secundum ASD and LAA percutaneous closure; 3) key steps of the procedural guidance emphasizing the role of 2-dimensional/3-dimensional transesophageal echocardiography; and 4) surgical closure of LAA and ASD. (J Am Coll Cardiol Img 2021;14:3–21) © 2021 Published by Elsevier on behalf of the American College of Cardiology Foundation.

Left atrial appendage (LAA) is a complex anatomic structure that derives from the embryological left atrium (LA). The remaining walls of the adult LA derive from an outgrowth of the pulmonary veins (1). Externally, the LAA lies anterior-lateral covering the atrio-ventricular groove, in close proximity to the left circumflex artery and the left pulmonary veins. Internally, LAA communicates with the atrial chamber through a relatively narrow, and oval-shaped ostium (Figure 1). Although each LAA is a unique anatomic entity that distinguishes each individual as a sort of fingerprint, the morphology of LAA may be roughly divided into 4 types: “chicken wing,” “cauliflower,” “cactus,” and “windsock” (2). Recognition of these morphological variations may be helpful in planning interventions. Figure 2 is a collage of different shapes of LAA visualized with 2-dimensional (2D) and 3-dimensional

(3D) transesophageal echocardiography (TEE) and volume-rendering reconstruction by cardiac computed tomography angiography (CCTA) (Central Illustration).

Notably, the orifice of LAA is laterally delimited by the so-called left lateral ridge (LLR) (3). This ridge separates the orifice of LAA from the left upper superior vein. The LLR is actually an infolding of the atrial wall, which contains epicardial adipose tissue and small vessels. Particular relevant for its electrophysiological implication is the vein or ligament of Marshall, which is located on the epicardial aspect of the LLR. This infolding may have different size and shape, and more frequently it almost virtually appears as a single muscular protuberance; in some cases, the LLR ends with a bulbus. At the beginning of the use of TEE, this bulbus was mistakenly diagnosed as a thrombus (which explains the name Coumadin

From the ^aCardiocentro Ticino Lugano, Lugano, Switzerland; ^bNew York University, New York, New York, USA; ^cVancouver General Hospital, Vancouver, Canada; ^dUniversity Hospital Liege, Liege, Belgium; ^eDepartment for Cardiac Surgery, Asklepios Klinikum Harburg, Hamburg, Germany; and the ^fMarcus Heart Valve Center Piedmont Heart Institute Atlanta, Atlanta, Georgia, USA. The authors attest they are in compliance with human studies committees and animal welfare regulations of the authors' institutions and Food and Drug Administration guidelines, including patient consent where appropriate. For more information, visit the [Author Center](#).

Manuscript received February 4, 2019; revised manuscript received June 6, 2019, accepted June 17, 2019.

**ABBREVIATIONS
AND ACRONYMS****2D** = 2-dimensional**3D** = 3-dimensional**AF** = atrial fibrillation**ASD** = atrial septal defect**CCTA** = cardiac computed tomographic angiography**FO** = fossa ovalis**IAS** = interatrial septum**IVC** = inferior vena cava**LA** = left atrium**LAA** = left atrial appendage**LLR** = left lateral ridge**MPR** = multiplanar reconstruction**SVC** = superior vena cava**TEE** = transesophageal echocardiography

ridge adopted by echocardiographers). **Figure 3** is a collage of different shapes of LLR visualized with 3D TEE and cardiac magnetic resonance.

PERCUTANEOUS CLOSURE OF LAA

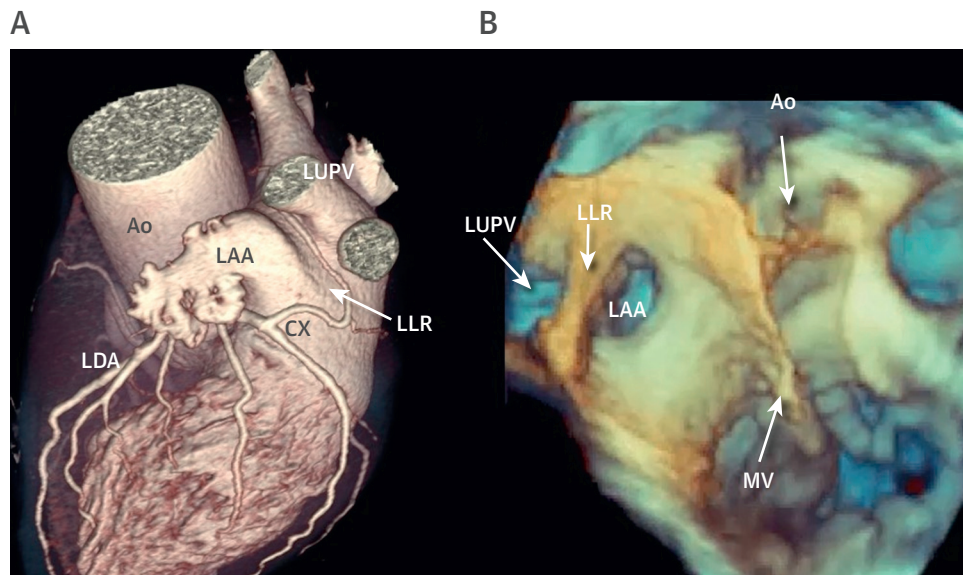
Atrial fibrillation (AF) is one of the most common arrhythmias, with a prevalence of 0.4% to 1% in adults 55 years of age or younger but up to 9% in individuals of 80 years or older (4). The most harmful complications of AF are the hemodynamic derangement and the risk of systemic emboli. This latter needs long-term anticoagulation therapy. However, a significant proportion of patients with AF have contraindications to anticoagulation. Thus, surgical or percutaneous closure of LAA have been proposed as nonpharmacological alternatives to anticoagulation (5,6).

Currently, 2 types of devices have been intensively studied and are available for percutaneous closure of LAA (7-9). The Watchman device (Boston Scientific, St. Paul, Minnesota) consists of a self-expanding

nitinol frame covered by a thin polyester membrane. Hooks around the mid-perimeter secure the device to the LAA wall. The device typically has to be 10% to 20% larger than the LAA body to have sufficient compression for stable positioning.

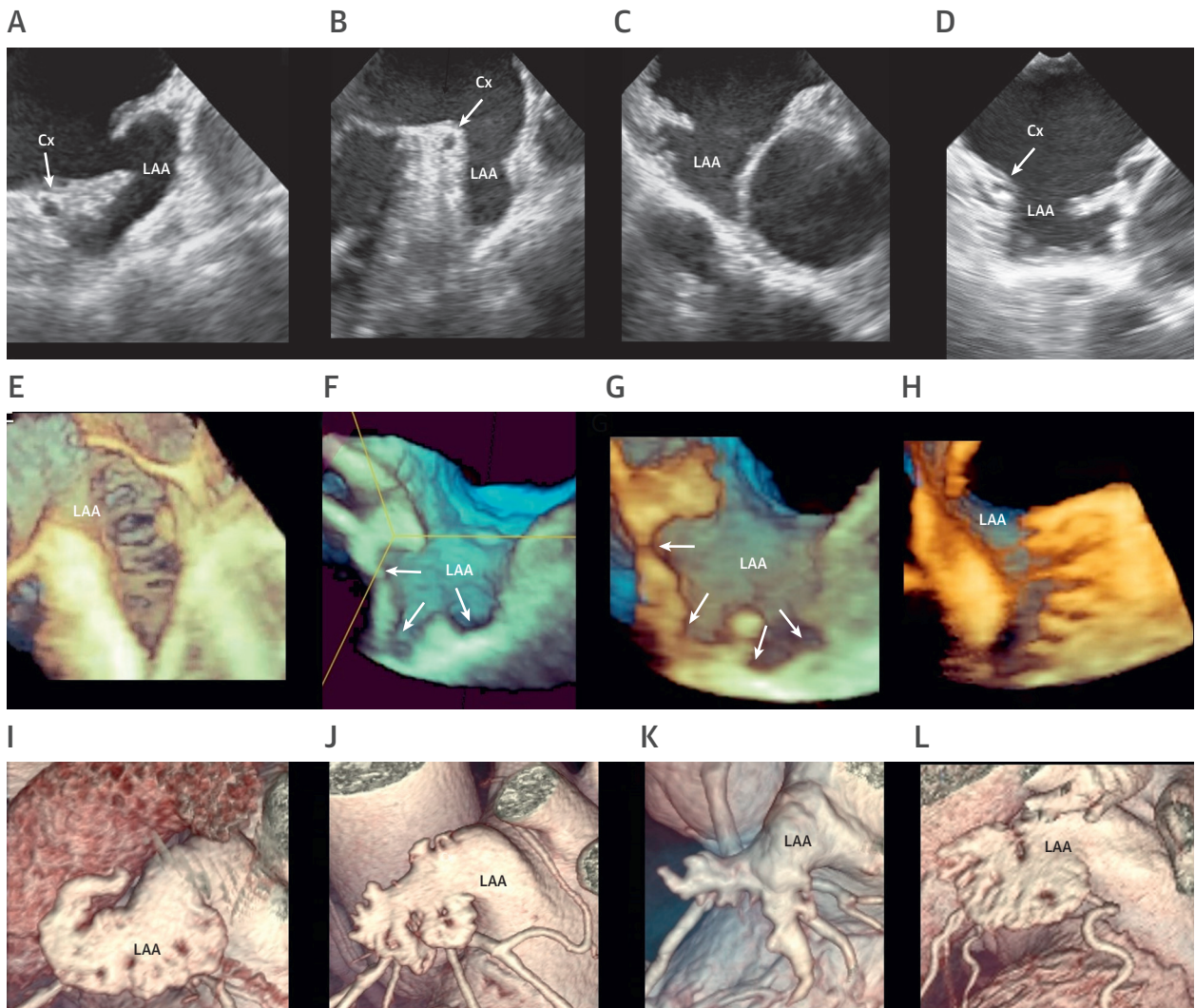
The Amplatzer Cardiac Plug consists of a distal lobe with a proximal disk connected by a flexible central waist. The lobe has stabilizing hooks to ensure retention and should be anchored in the 'landing zone,' which is approximately 1 cm distal to the LAA orifice. The disc fully covers the orifice, thereby enabling re-endothelialization from the surrounding atrial wall. The second-generation of the Amplatzer Cardiac Plug (called Amulet) was redesigned for LAA to be more stable by being stiffer with a wider lobe, more hooks, and options for more sizes.

PRE-PROCEDURAL ASSESSMENT. The key elements for LAA closure baseline imaging include ruling out LAA thrombus, providing detailed characterization of the LAA anatomy, and measuring the LAA orifice and depth. Both TEE and CCTA are well suited for pre-procedural imaging. TEE is the traditional modality for preimaging, however, there are several advantages with CCTA that make it the preferred modality,

FIGURE 1 Position of LAA

Anatomic relationships of LAA with surrounding structures from (A) an external and (B) an internal perspective. Ao = aorta; CX = circumflex artery; LAA = left atrial appendage; LDA = left anterior descending artery; LLR = LLR = left lateral ridge; LUPV = left upper pulmonary vein; MV = mitral valve.

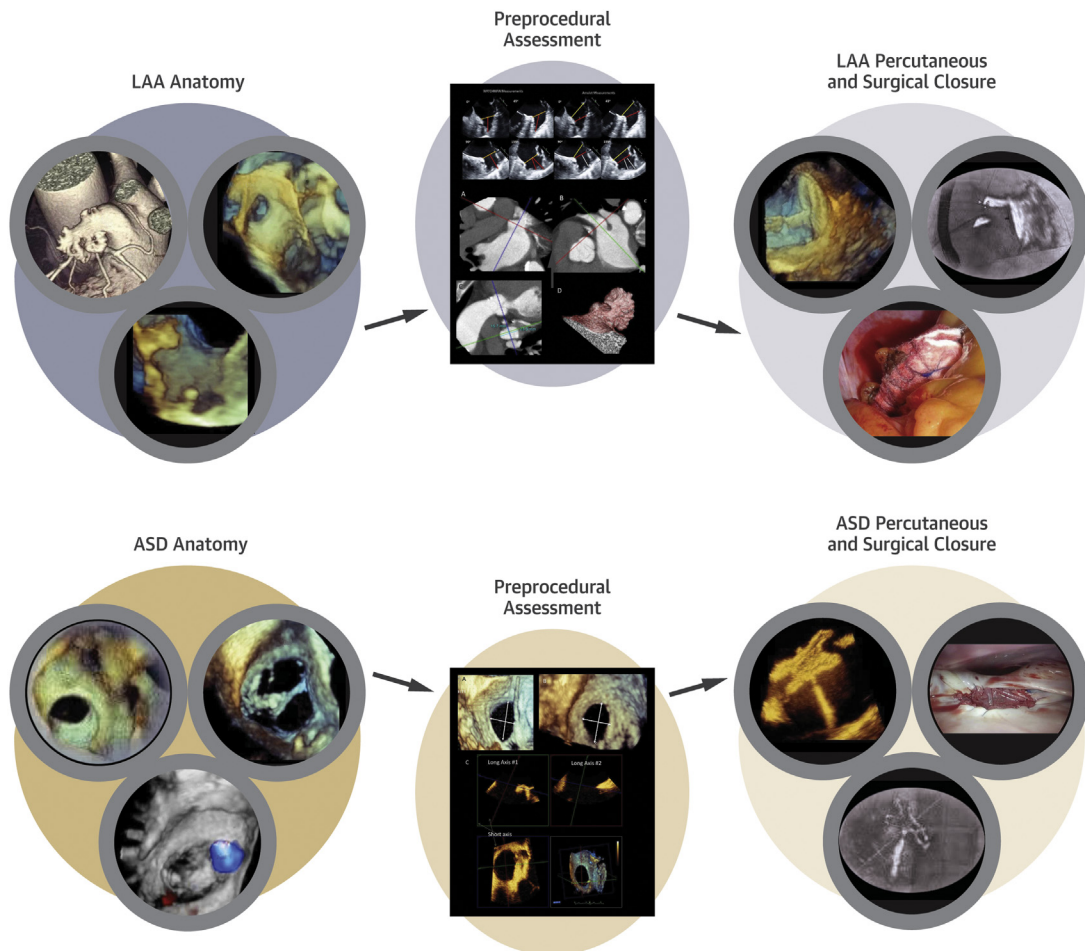
FIGURE 2 Images of LAA



The complex and variable anatomy of LAA as visualized using 2D TEE (A to D; arrows point at the circumflex artery), 3D TEE (E to H; arrows point at lobes), computed tomography (I to L). 2D = 2-dimensional; CX = circumflex artery; TEE = transesophageal echocardiography; other abbreviations as in Figure 1.

including noninvasive acquisition, higher spatial resolution to characterize LAA anatomy, and more accurate sizing. The advantages of TEE include being widely available and being the default procedural imaging guidance in most centers for LAA closure, thus, it can be performed in the catheterization laboratory prior to venous access, without the additional cost, radiation, and contrast administration (although this risks procedural cancellation if there is LAA thrombus or unsuitable anatomy).

2D TEE is the current gold standard to rule out LAA thrombus. In the setting of dense spontaneous echo contrast, giving microbubble ultrasonic enhancement agents may help delineate the presence of sludge or thrombus. CCTA performed with protocol adaptations (e.g., delayed imaging, dual-enhanced scan, prone positioning, dual-energy source) can achieve high positive predictive values and specificities >90%, and negative predictive values and sensitivities close to 100%, to rule out LAA thrombus.

CENTRAL ILLUSTRATION Role of Imaging Modalities in LAA and ASD Percutaneous and Surgical Closure

Faletra, F.F. et al. *J Am Coll Cardiol Img.* 2021;14(1):3-21.

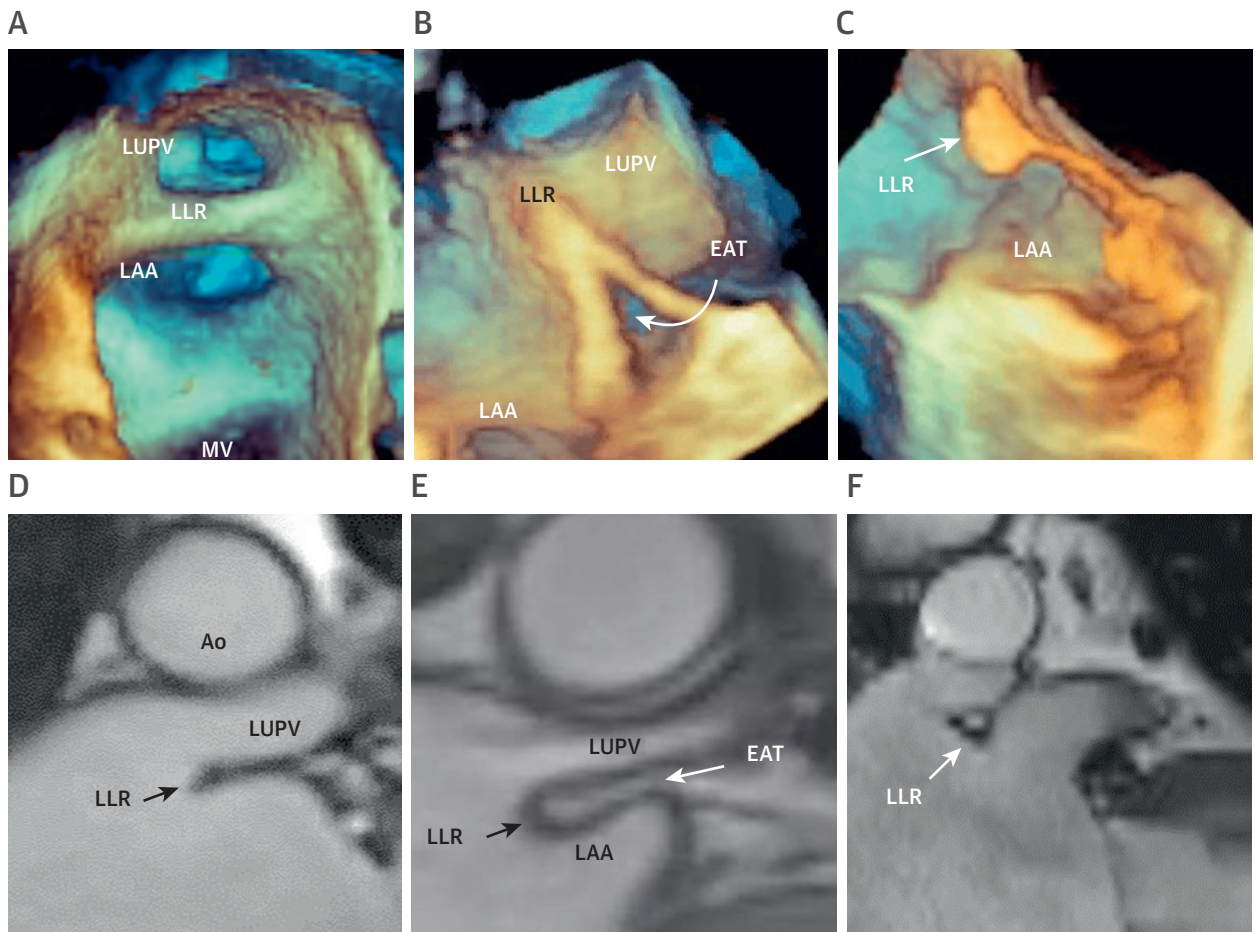
Comprehensive images showing ASD and LAA anatomy, pre-procedural assessment, and percutaneous and surgical procedures. ASD = atrial septal defect; LAA = left atrial appendage.

Detailed characterization of the shape of the LAA body and orifice is important to guide device selection and sizing. The presence and location of chicken wing angulation, bifurcation into lobes, and presence of trabeculations and pectinate ridges can influence the site of device implantation and the device type selection. Envisioning how the devices can fit within the LAA anatomy allows choosing the optimal device, and specifies the site of sizing measurements. For 2D TEE, the probe should be positioned at the mid-esophagus, LAA interrogated from 0 to 135° and images recorded in at least 4 views (0, 45°, 90°, and 135°). For CCTA, the LAA should be visualized with oblique multiplanar reconstructions (MPRs) and, 3D

volume-rendering reconstructions. Proximity to surrounding structures such as the left upper pulmonary vein, mitral annulus, and pulmonary artery should be assessed. The trajectory (e.g., superior-anterior, inferior-anterior, or rightward superior) of the proximal neck and body of the LAA should be determined on 2D TEE or CCTA to guide sheath selection and location of trans-septal puncture.

The specific locations to measure the LAA ostium and depth can be different depending on the devices, and the manufacturers' instructions for use should be followed. For Watchman, the LAA ostium is measured from the circumflex artery to a superior point 1 to 2 cm inside the LLR, and the LAA depth is measured

FIGURE 3 Images of LLR

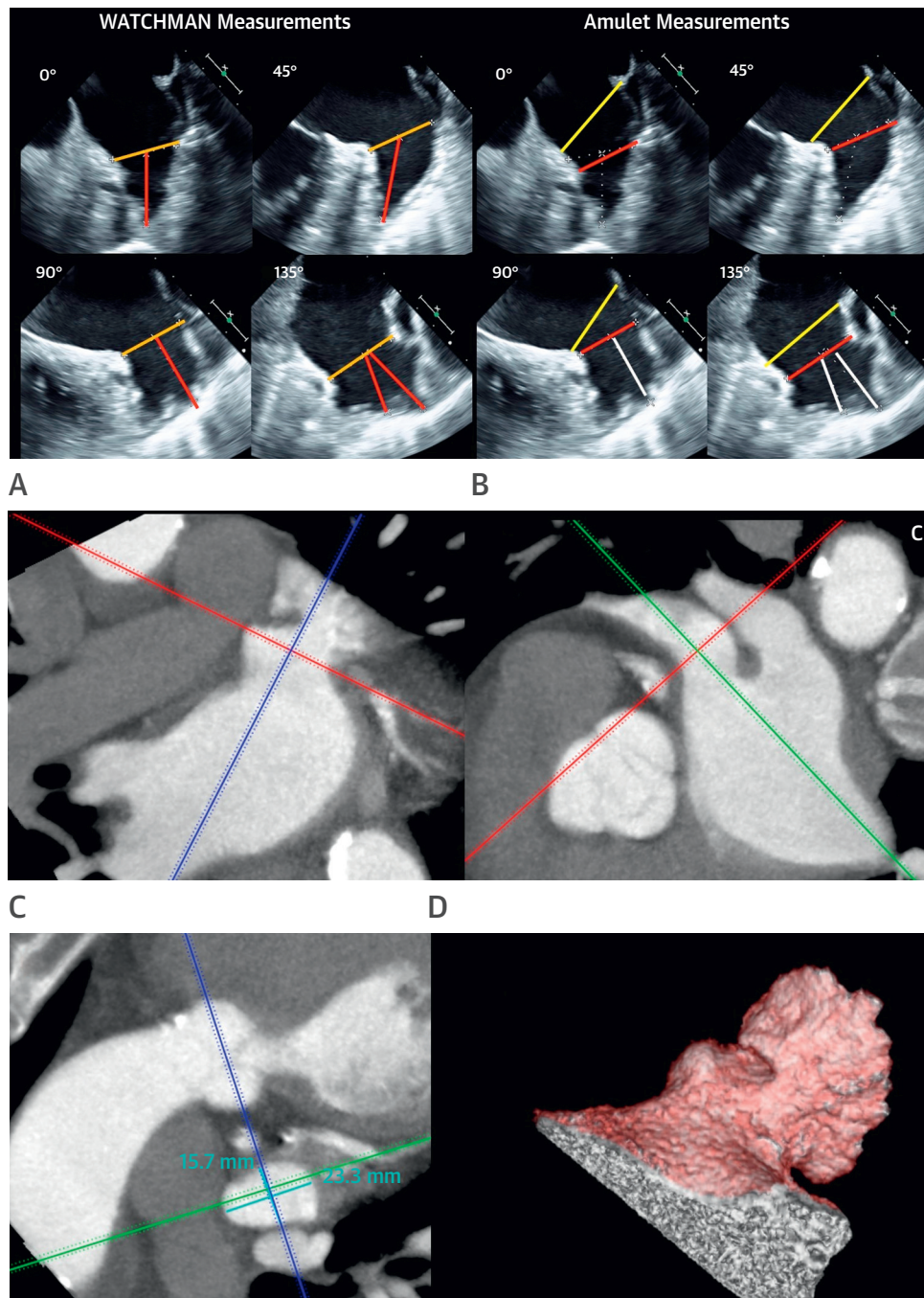


Different shapes of LLR as visualized using 3D TEE (**A to C**) and cardiac magnetic resonance (**D to F**). **A and E** clearly show that the LLR is actually an infolding of the left atrial wall occupied by EAT. **A and D** show that this infolding can be almost virtual and it is visualized as a single muscular protuberance. **C and F** show that the LLR may end with a bulbus taking the name of Q-tip sign. 3D = three-dimensional; EAT = external adipose tissue; LLR = left lateral ridge; LUPV = left upper pulmonary vein; MV = mitral valve; other abbreviations as in [Figure 2](#).

from this line to the tip of the LAA ([Figure 4](#), left panel). For Amplatzer Amulet, the orifice is measured from the inferior LAA edge to the left upper pulmonary vein ridge superiorly, and the landing zone diameter is measured 10 to 12 mm inside the orifice ([Figure 4](#), right panel). Measurements on 2D TEE should be measured at end-systole (cardiac phase with the largest dimension) at 4 angles (0, 45°, 90°, and 135°). 3D assessments should also be done on TEE to understand the shape of the orifice, and the maximum and minimum diameters should be measured. Measurements on CCTA should be performed at late atrial diastole corresponding to 30% to 40% of the RR interval, where the LAA dimension is largest. Using MPR, an oblique view of the LAA ostium is selected where the circumflex artery, the

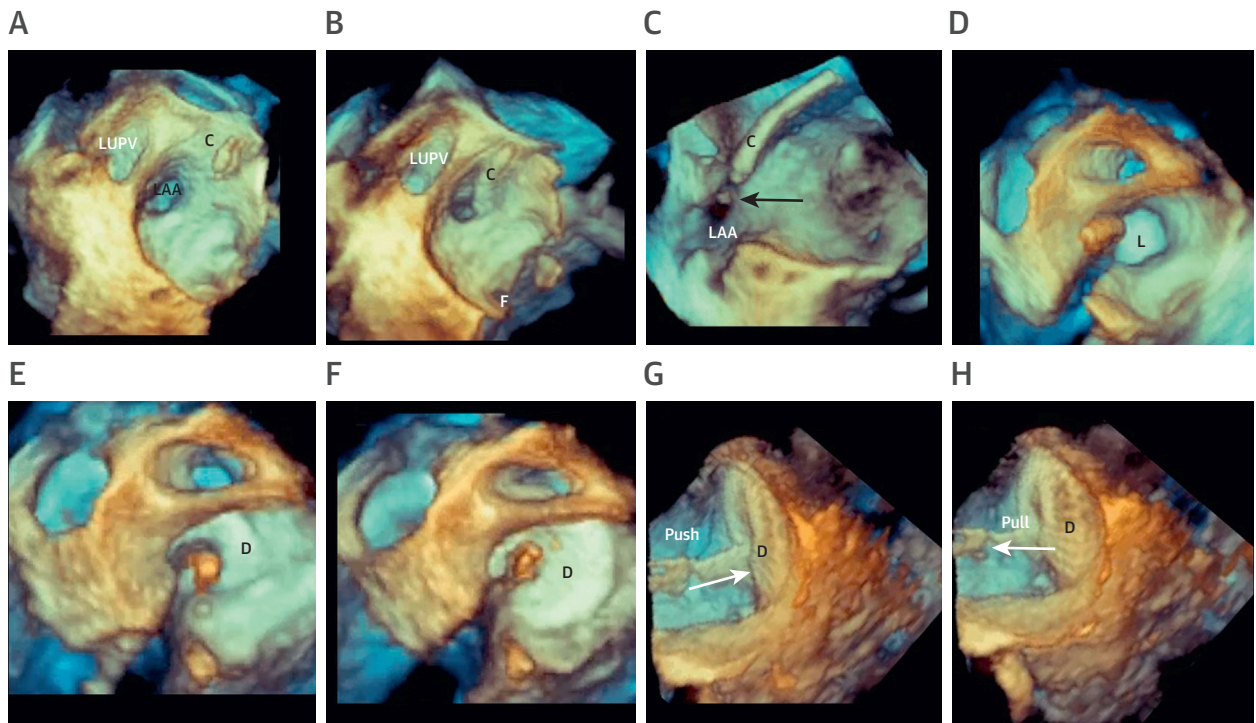
LLR, and the LAA are well shown. The cross-hairs are coaxially adjusted to the LAA wall in this plane, and in another orthogonal cross section of this plane. After double-oblique adjustments, the third orthogonal “enface” view is used to measure the maximum and minimum dimensions of the LAA ostium ([Figures 4A to 4D](#)). The depth of the LAA can be measured on MPR or maximal intensity projections (especially if there are sharp angulations).

INTRAPROCEDURAL GUIDE. The ideal location of the trans-septal puncture is in the inferior-posterior portion of the fossa ovalis (FO), which allows coaxial engagement of the LAA, thus minimizing the risk of perforation. Once trans-septal access is obtained, a guide catheter is gently advanced to

FIGURE 4 Assessing LAA Size

(Left) Watchman measurements (**dotted white lines**) at 4 angles, for the LAA ostium and depth. **(Right)** Amplatzer Amulet measurements at 4 angles, with **yellow lines** measuring the LAA orifice, and the **red lines** measuring the landing zone at 12 mm within the orifice. CCTA measurements of the LAA: **(A)** oblique plane with adjustment of the cross-hair to be coaxial to the wall of the LAA, **(B)** 2nd oblique plane with the adjustment of the cross-hair to be coaxial to the wall of the LAA, **(C)** double-oblique en face plane allowing measurement of the maximum and minimum diameter of the LAA, and **(D)** 3D volume-rendered projection of the LAA showing proximal angulation, and trabeculations in the mid to distal body of the LAA. CCTA = cardiac computed tomographic angiography; other abbreviations as in [Figures 1 and 3](#).

FIGURE 5 Steps of LAA Closure



Sequential steps of the LAA occlusion. (A to C) The catheter (C) is advanced to engage the LAA. (D) The lobe (E) is expanded. (F) The disk is expanded. (G to H) Push and pull maneuver. C = catheter; D = disc; L = lobe; other abbreviations as in Figures 1 and 3.

engage the LAA. The correct position of the guide catheter inside the LAA is usually confirmed using 2D/3D TEE. The next step is the deployment of the device. This maneuver is guided by 2D/3D TEE, which may follow the device progressively expanding into the LAA (Figures 5A to 5F). 2D TEE color Doppler is used to evaluate the presence and severity of peri-device leak. Once the optimal device positioning is confirmed, a pull-push maneuver assures that the device is firmly anchored (Figures 5G and 5H). Then, as the last step, the delivery system is withdrawn.

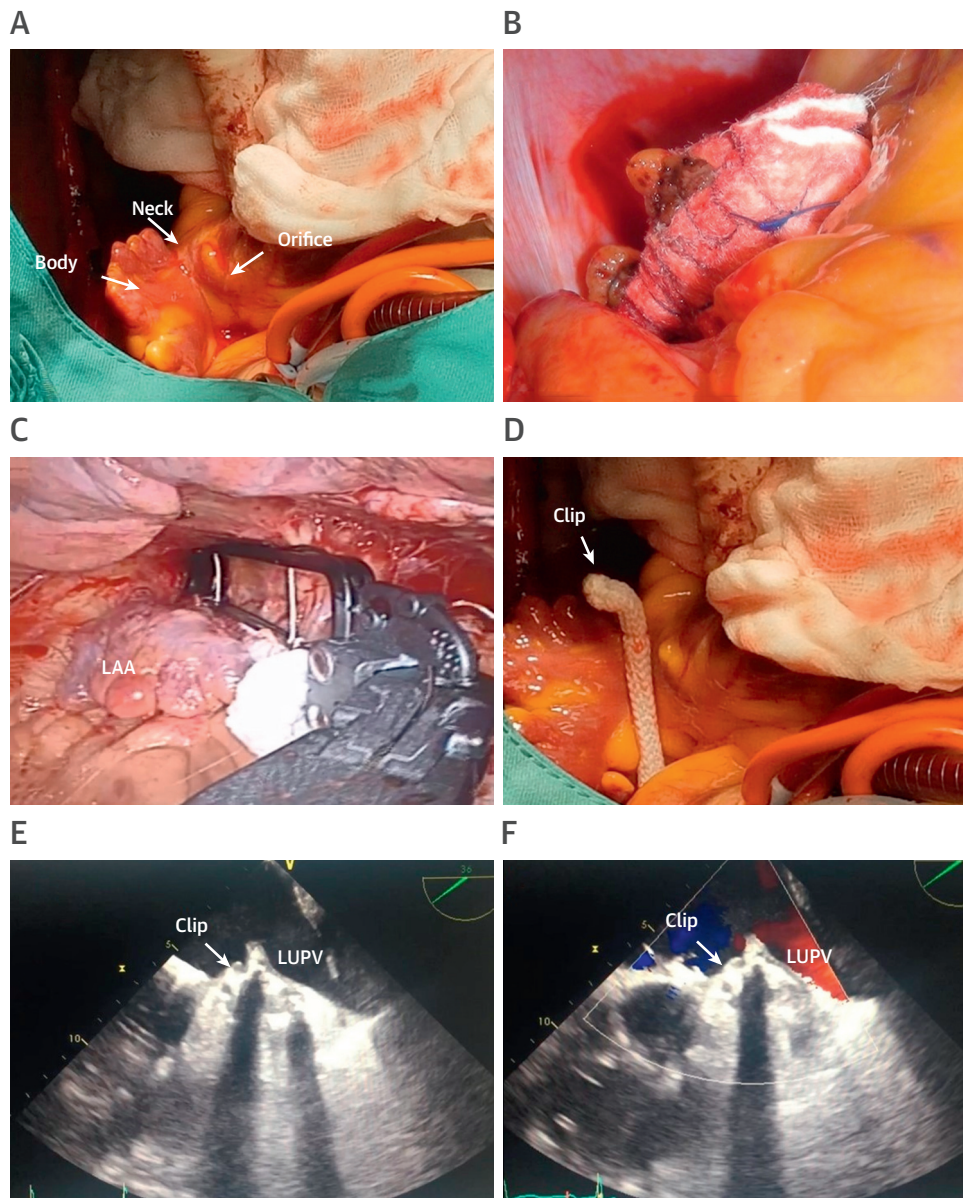
PROCEDURAL AND POST-PROCEDURAL COMPLICATIONS.

During the opening into the LAA, the device can slide out of the border of the LAA. In such a case the device must be repositioned. Peri-device leak is one of the controversial issues of percutaneous closure of LAA. Indeed, despite the existence of peri-device leak, the PROTECT-AF (Percutaneous Closure of the Left Atrial Appendage Versus Warfarin Therapy for Prevention of Stroke in Patients With Atrial Fibrillation) cohort, left atrial appendage occlusion was demonstrated to be non-inferior to warfarin and

resulted in a statistically significant improved clinical outcome compared with warfarin at long-term follow-up. Moreover, criteria to classify the size of the residual leak (<3 mm or <5 mm) are elusive and arbitrary until this parameter is assessed with consistent methodology. Following percutaneous LAA closure, the incidence of device-related thrombus is <5% but it is associated with higher risk of stroke and systemic embolism. In such a case, periodic TEE should be considered, and anti-coagulation should promptly be resumed until the thrombus disappear.

SURGICAL CLOSURE

Surgical exclusion of the LAA can be achieved either endocardially or epicardially by over-sewing, resection, ligation, stapling (with or without amputation), or using a clip system (Atriclip LAA exclusion system, AtriCure, Mason, Ohio) inserted at the base of the LAA (10). These LAA exclusion procedures are mostly performed in association with other open chest cardiac surgery interventions. However, the surgical

FIGURE 6 Surgical Closure

(A) Intraoperative view of LAA. **(B)** Excised LAA, closure with a 2-layer felt supported suture technique. **(C)** Intraoperative LAA clip closure during stand-alone epicardial off-pump beating heart procedure. **(D)** Intraoperative view of clipped LAA with an AtriClip device. See [Videos 1 and 2](#). **(E and F)** 2D TEE intraoperative monitoring showing a good result of the procedure. The absence of pouch of residual flow through LAA remnant is documented. See [Video 3](#). Abbreviations as in [Figures 1 to 3](#).

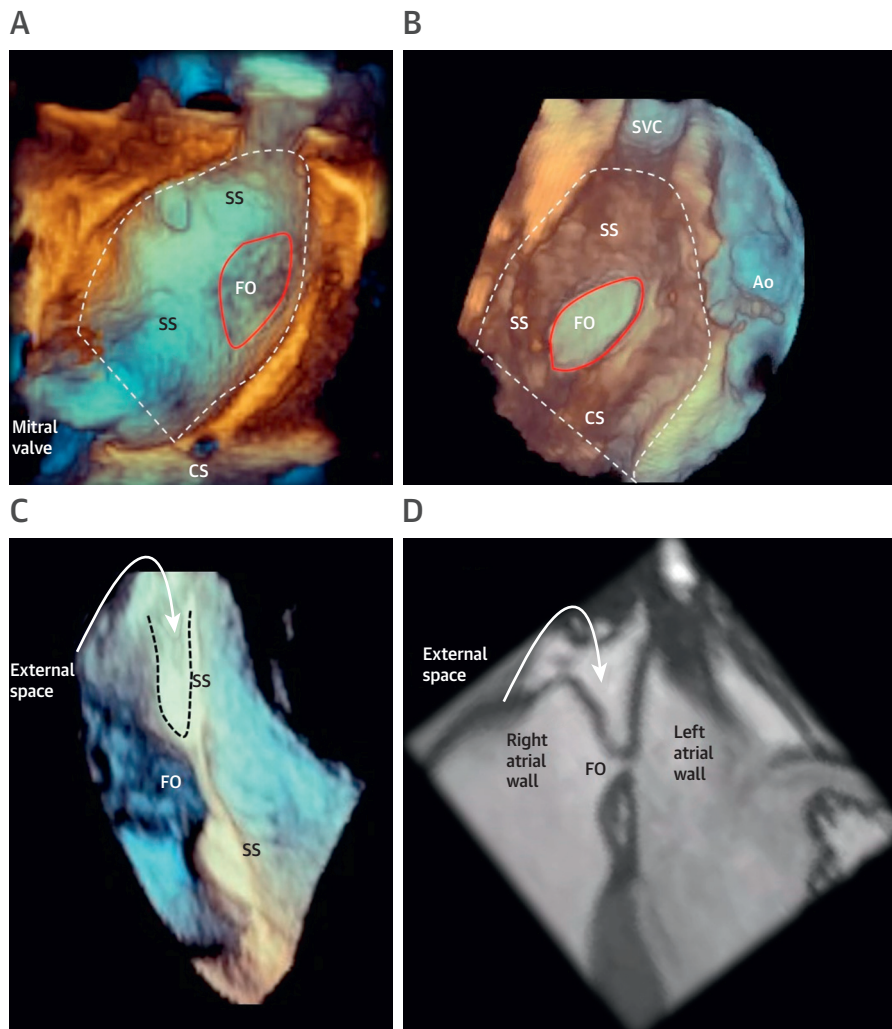
LAA closure can also be performed as a pure stand-alone procedure, either minimal invasively (mini thoracotomy) or thoroscopically.

When performing the excision technique, it is mandatory to cut the LAA down to the base and then close the incision in a double layer fashion, either

with or without pericardial or felt strip because this region of the heart is difficult to reach once the cardiopulmonary bypass is off ([Figure 6B](#)).

The AtriCure LAA exclusion system, a nitinol-based clip surrounded by a cotton scarf, was designed to close the LAA at the base with equal force

FIGURE 7 Anatomy of IAS



(A, B) 3D TEE images of the IAS seen “en face”. The IAS appears as an extensive surface (white dotted line) either from the left (A) or from the right (B) perspectives. However, the so-called SS is actually an infolding of the atrial wall occupied by external adipose tissue (curved arrows) as visualized with 3D TEE in cross section (C) or with cine cardiac magnetic resonance (D). The FO (red line) is the area corresponding at the “true” IAS. Indeed, puncturing or removal the FO creates a direct interatrial communication, whereas puncturing or removal the SS creates an exit into the external space. Ao = aorta; CS = coronary sinus; FO = fossa ovalis; IAS = interatrial septum; SS = septum secundum; SVC = superior vena cava; other abbreviations as in Figures 2 and 3.

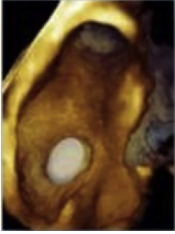

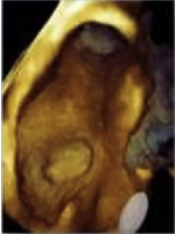
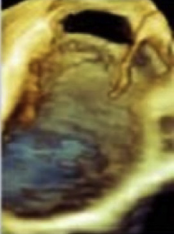
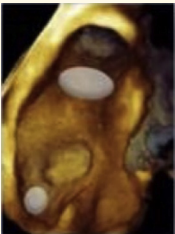
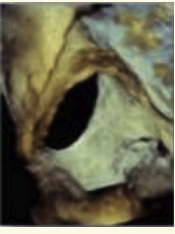
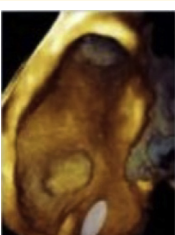
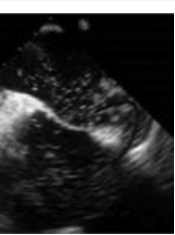
distribution over the complete length of the clip. In case of a pouch remnant >5 mm, the device needs to be repositioned until a pouch <5 mm is documented in TEE (Figures 6C and 6D, Videos 1 and 2). Intra-operative TEE during cardiac surgery is important (Figures 6E and 6F, Video 3). In case of an arrested heart, visual control of complete closure is feasible, but TEE assessment before going off-pump is essential because at this time it is still possible to correct a possible failure. In case of a beating heart approach,

TEE assessment must be on-line to allow a possible correction.

ATRIAL SEPTAL DEFECT PERCUTANEOUS AND SURGICAL CLOSURE: ANATOMY OF INTERATRIAL SEPTUM

The interatrial septum (IAS) is defined as a partition interposed between right atrium and LA; puncturing or removal of IAS must create a direct

TABLE 1 Different Types of ASD

Type	Prevalence	Site	Image
Secundum ASD	70%		
Primum ASD	15-20%		
Sinus Venous ASD	5-10%		
Unroofed coronary sinus	<1%		

ASD = atrial septal defect.

communication between the 2 atria. According to this definition, the “true” IAS corresponds to the floor of the FO of the embryonic “septum primum.” The muscular area surrounding the FO and known as “septum secundum” is an enfolding of atrial wall that starts anteriorly and superiorly between the orifice of superior vena cava (SVC) and the right pulmonary veins and extends posteriorly and inferiorly. This infolding is occupied by external adipose tissue (11) (Figure 7).

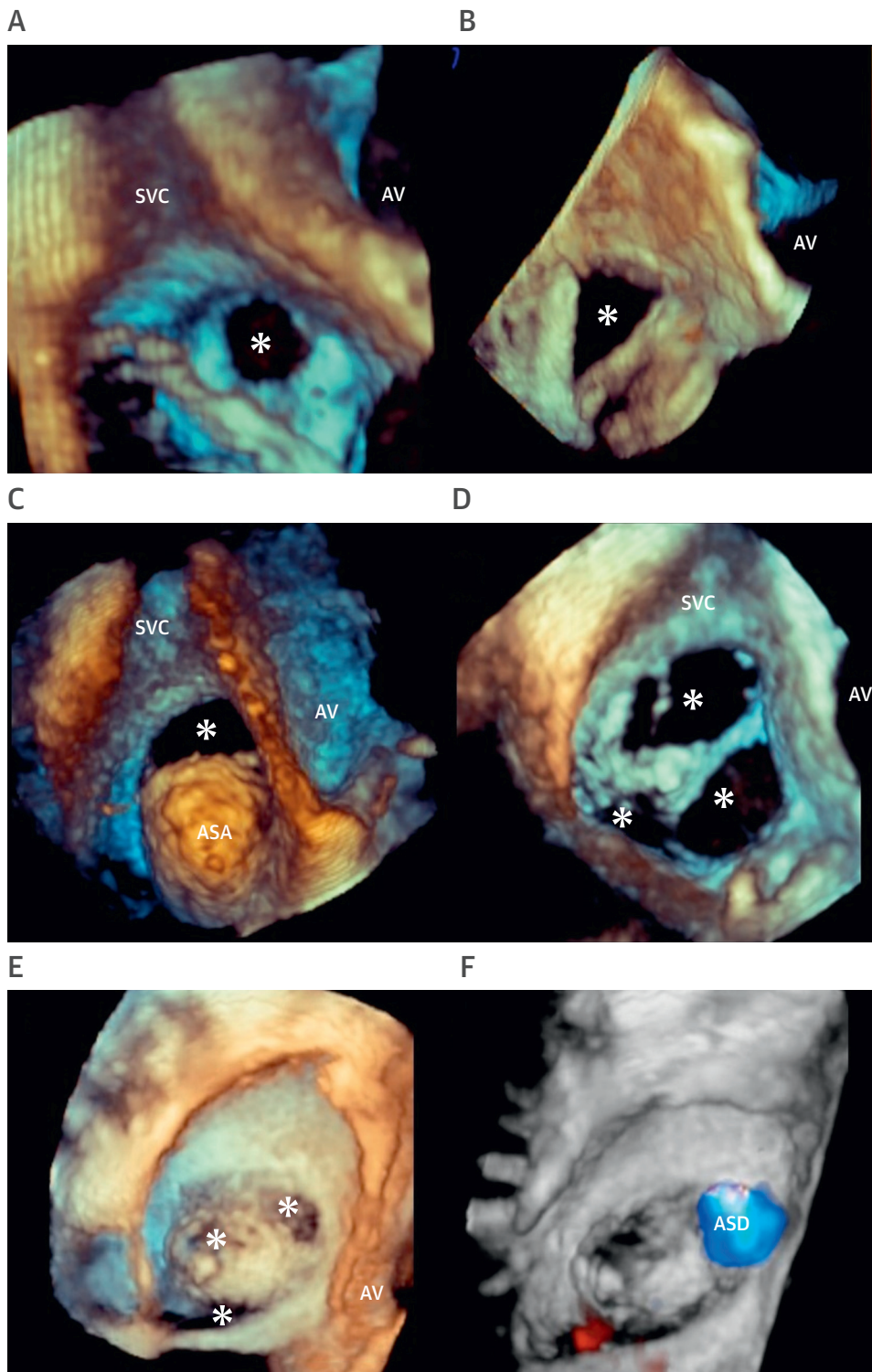
ANATOMY OF ATRIAL SEPTAL DEFECTS

Excluding the bicuspid aortic valve, atrial septal defect (ASD) is the most common congenital cardiac

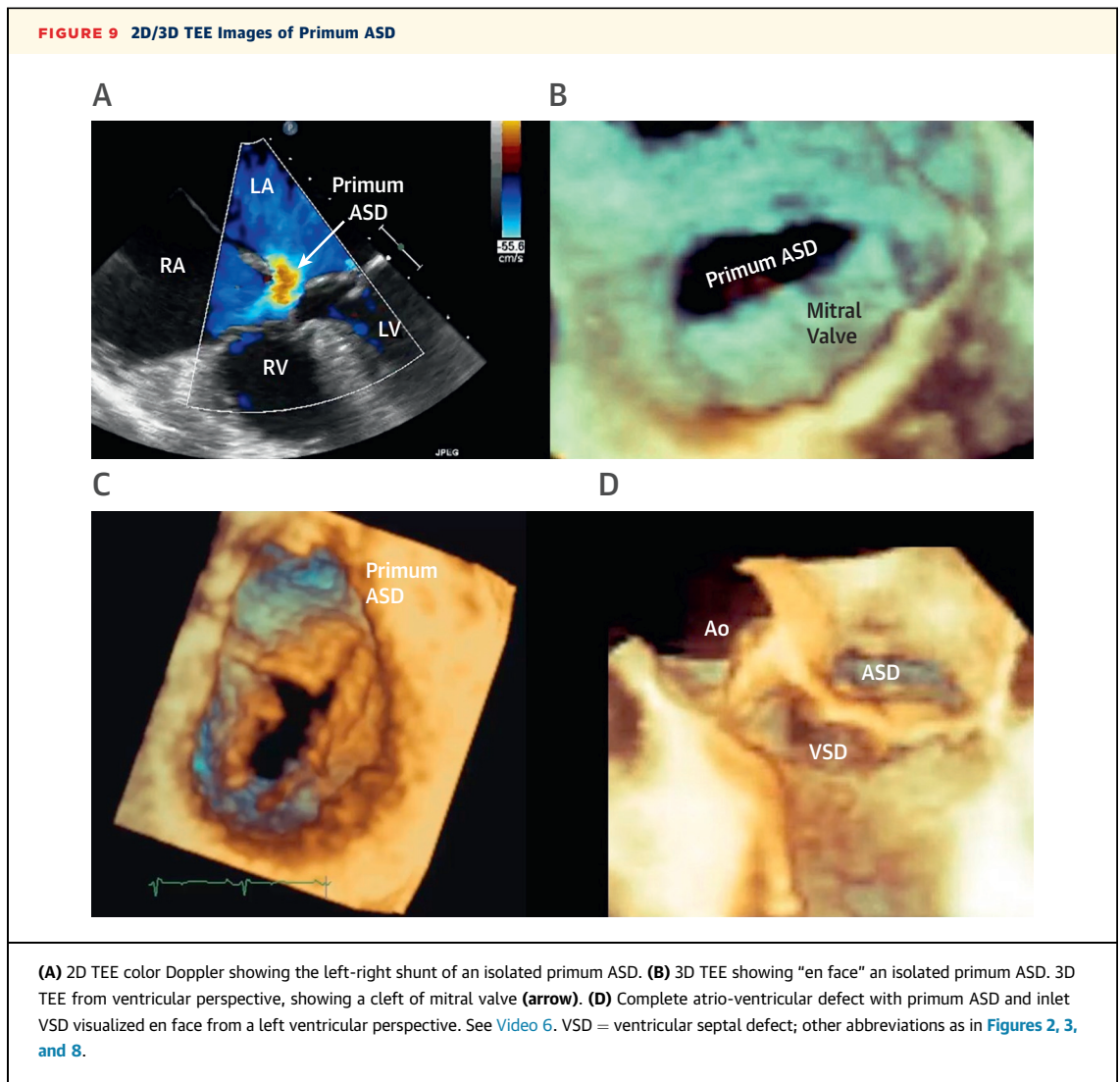
anomaly in adults with an approximate prevalence of 1 of 1,000 individuals (12). There are 4 main types of ASDs, listed in decreasing frequency: secundum ASD, primum ASD, sinus venosus ASD, and unroofed coronary sinus (Table 1).

Secundum ASD is the most common type, accounting for about $\frac{3}{4}$ of all ASDs, and is twice as common in females than males. It is located within the borders of the FO and its size varies from a few millimeters in diameter to an almost complete absence of the FO. As revealed by 3D TEE, secundum ASD may be circular, ovoid, triangular, or irregular in shape. Its orifice may be solitary or may be fenestrated with multiple openings (Figures 8A to 8D). Drop-out artifacts (due to the thinness of the FO and

FIGURE 8 Images of Ostium Secundum ASD



(A to D) 3D TEE images of different size, shape, and number of ASD (asterisks). **(E, F)** Drop-out artifacts may look like additional ASDs (asterisks). In such a case, 3D color Doppler helps to distinguish the true defect from the drop-out artifacts by delineating with the color the borders of the ASD. See [Video 5](#). ASD = atrial septal defect; AV = aortic valve; LA = left atrium; LV = left ventricle; RA = right atrium; RV = right ventricle; other abbreviations as in [Figures 2, 3, and 7](#).



its oblique position to the ultrasound beam) are not infrequent and may look like additional ASD (13). In such a case 3D color Doppler may help in delineating the borders of the true ASD (Figures 7E and 7F).

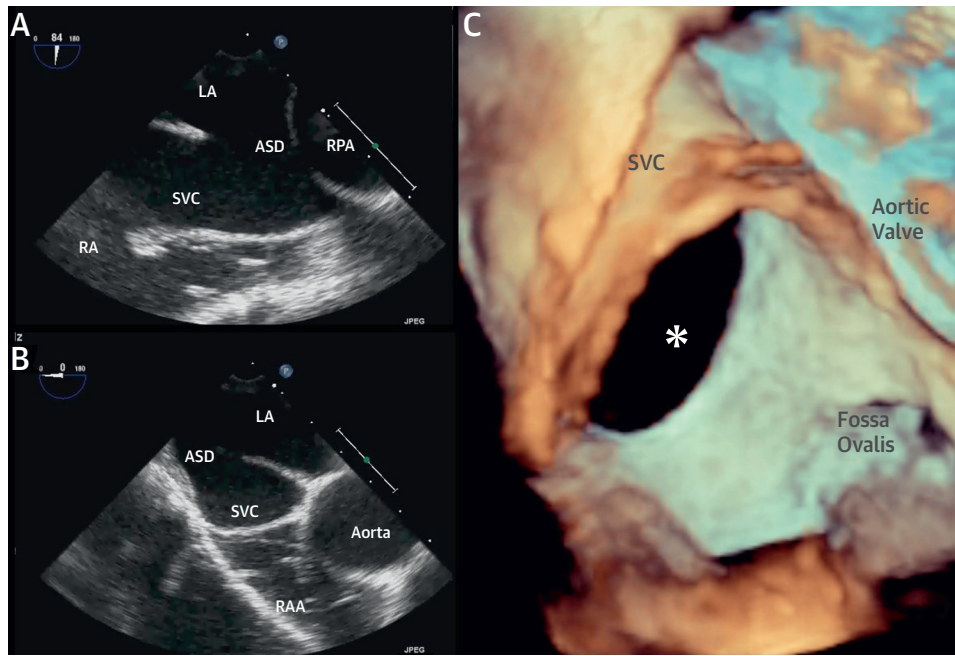
Primum ASD (atrio-ventricular septal defect) accounts for about 15% to 20% of all ASDs and it is usually part of a larger endocardial cushion defect spectrum (Figure 9, Videos 5 and 6).

Sinus Venosus ASDs are relatively rare (5% to 10% of all ASDs) and are located at the interface between the right atrium and the embryological sinus venosus. About $\frac{2}{3}$ of such defects occur near the SVC and the remaining $\frac{1}{3}$ next to the inferior vena cava (IVC) (Figure 10, Videos 7 and 8). The SVC type of sinus venosus ASD is typically associated with anomalous drainage of the upper and middle pulmonary vein into the right atrium or the SVC.

Unroofed Coronary Sinus is the rarest form of ASD (<1% of all ASDs). Fenestrations in the roof of the coronary sinus allow for drainage of left atrial blood into the right atrium via a dilated coronary sinus ostium. When such a defect is associated with persistent left SVC it is referred to as Raghbi syndrome (Figure 11, Video 9).

PRE-PROCEDURAL ASSESSMENT. At present only the secundum ASD is amenable to percutaneous closure. Echocardiography is the primary means of establishing the diagnosis of an ASD. Cardiac catheterization, CT, and cardiac magnetic resonance may provide additional hemodynamic data and visualization of associated anomalies. The role of imaging is to establish: 1) type of ASD; 2) size of ASD and its rims; 3) hemodynamic consequences including shunt direction, right heart dilatation, and the degree of

FIGURE 10 2D/3D TEE Images of Sinus Venus ASD

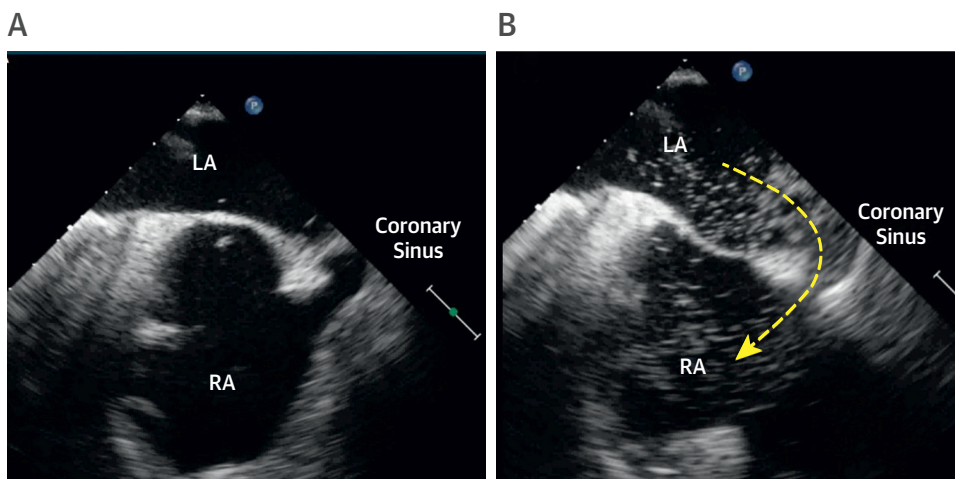


Sinus venus ASD in long (A) and in short (B) axis SVC. (C) 3D TEE from right side perspective showing the sinus venus ASD (asterisk) in "en face" view. See Videos 7 and 8. RAA = right atrial appendage; RPA = right pulmonary artery; other abbreviations as in Figures 2, 3, 7, and 8.

pulmonary hypertension and pulmonary vascular resistance; and 4) presence or absence of contraindications for ASD closure including associated anomalies.

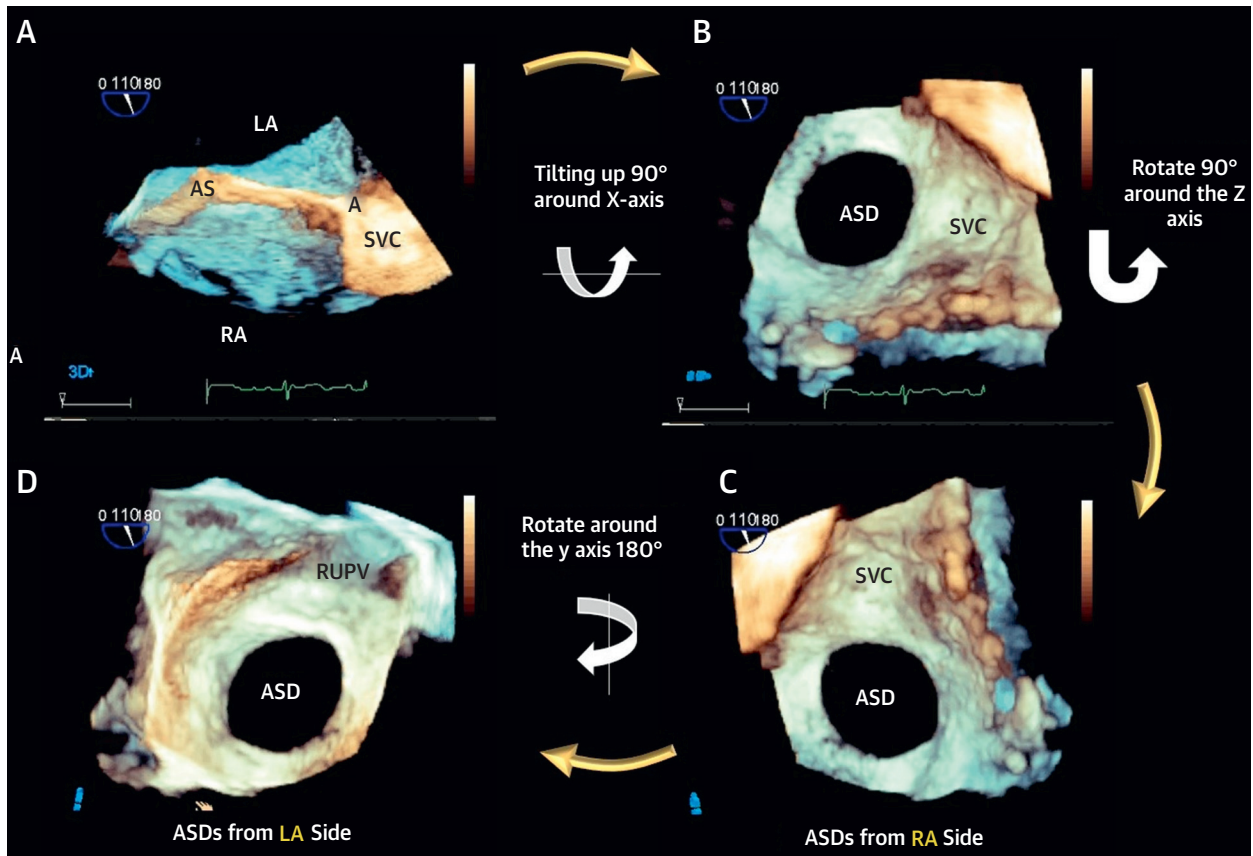
Although the basic diagnosis of an ASD and its hemodynamic consequences can be established using 2D TTE in many instances, 2D and 3D TEE are needed for detailing the ASD anatomy and sizing. 3D TEE

FIGURE 11 2D TEE Images of Unroofed Coronary Sinus



Unroofed coronary sinus seen (A) in 2D TEE and (B) confirmed using the contrast. See Video 9. Abbreviations as in Figures 2 and 8.

FIGURE 12 A "Turple" Maneuver



This maneuver allows one to align the ASD and surrounding structures in a correct anatomic orientation. See [Video 4](#). RUPV = right upper pulmonary vein; other abbreviations as in [Figures 7 and 8](#).

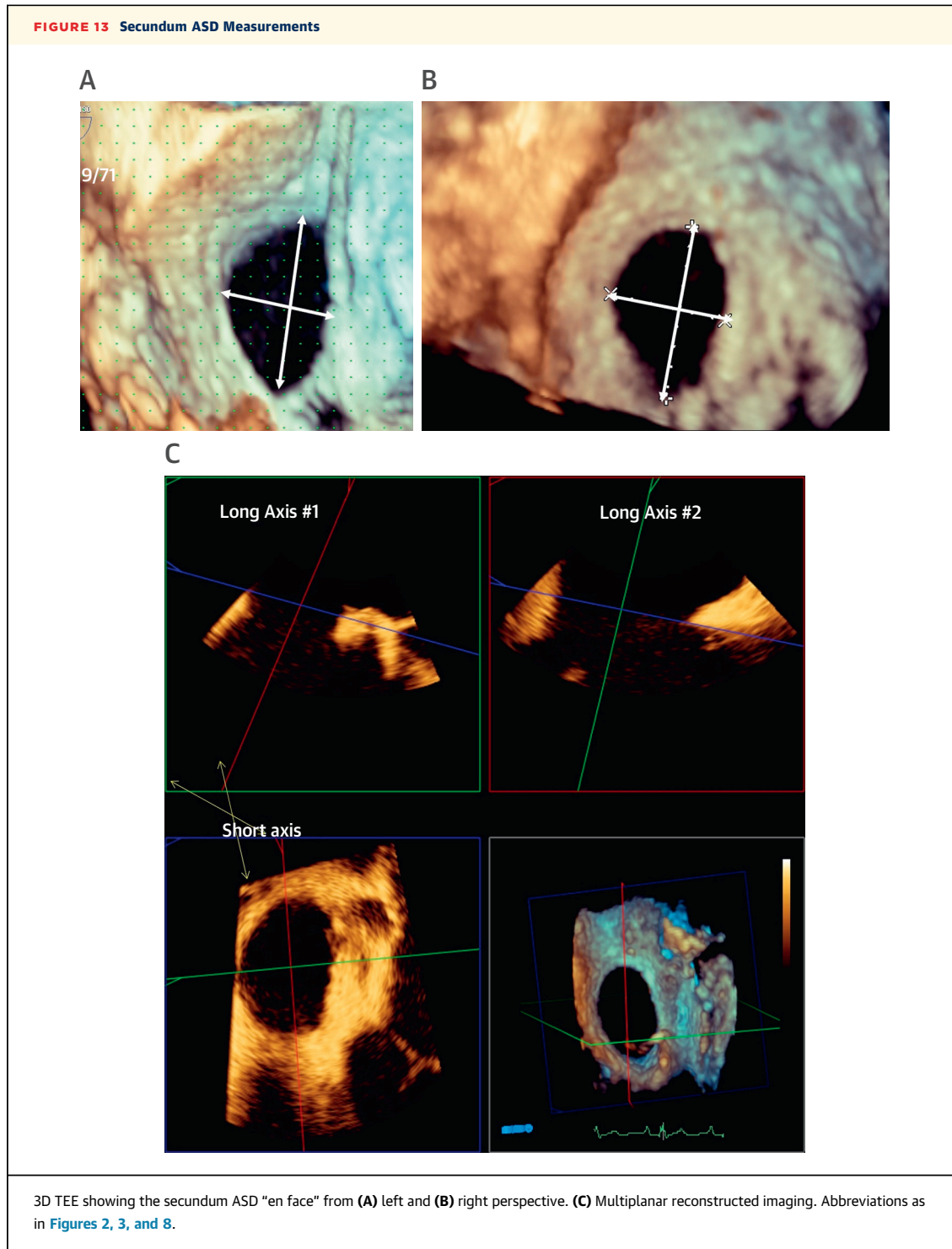
overcomes many limitations of 2D TEE by allowing for accurate visualization of the size and shape of the defect and its rims on unique en face views of the ASD. Anatomically correct orientation of 3D TEE images is essential for the diagnosis of any ASD. A Tilt-Up-Then-Left maneuver has been developed to aid in anatomically orienting ASD images on 3D TEE ([Figure 12](#), [Video 4](#)).

Proper ASD sizing is essential for both surgical and percutaneous ASD closure. Correct percutaneous device size selection avoids complications such as incomplete defect closure, device embolization, and disc erosion into surrounding cardiac structures due to either an undersized or oversized closure device. It is important to make a distinction between a maximum ASD diameter measured on pre-procedural imaging (referred to as

'unstretched diameter') and the intraprocedurally measured maximum ASD diameter (referred to as 'stretched diameter') using a balloon sizing technique by gradually inflating a sizing balloon placed across an ASD until no color Doppler flow across the ASD is seen on TEE. Amplatzer device selection is based on either the measured stretched diameter or by adding 6 to 8 mm to the unstretched diameter.

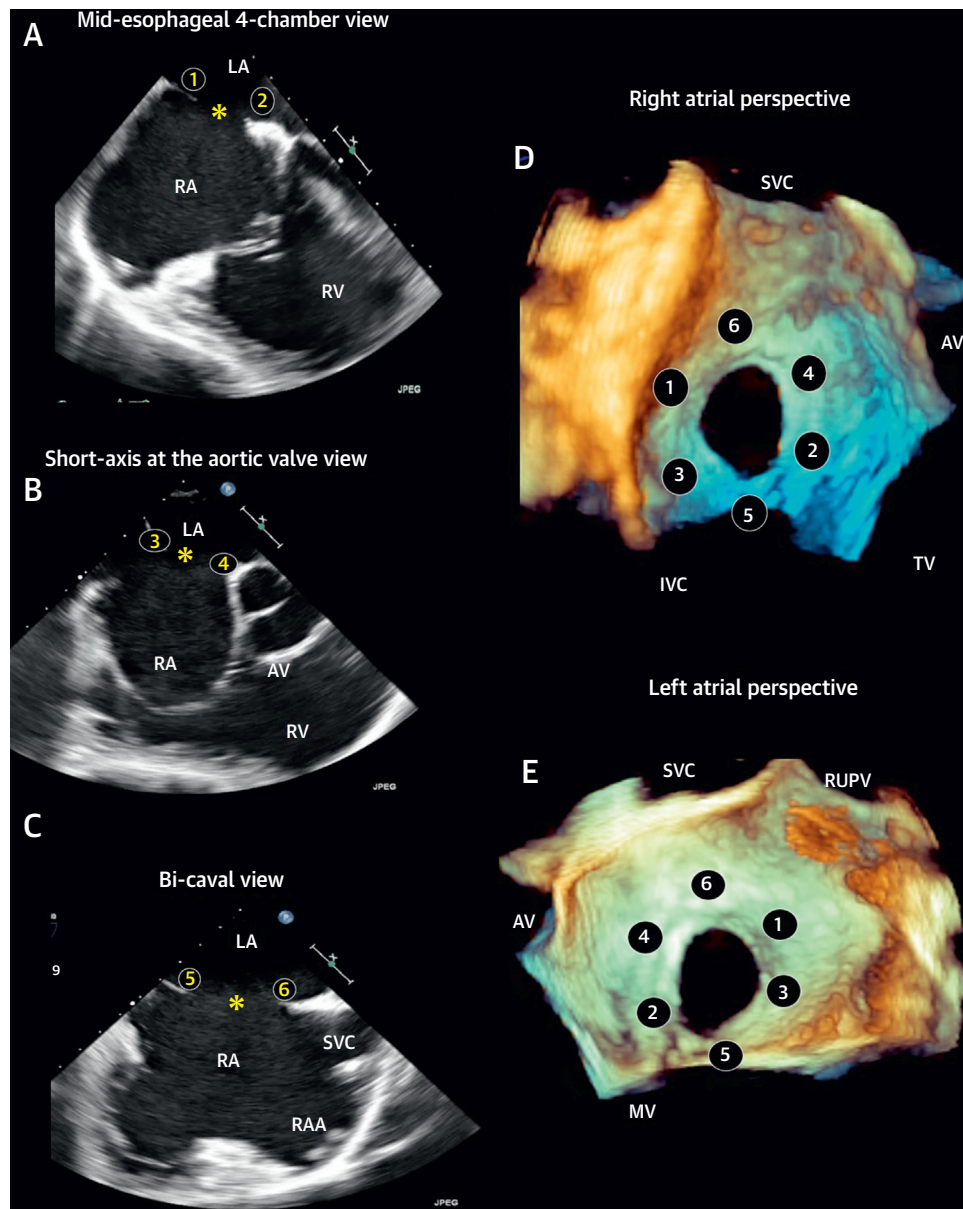
Sizing may be done directly on volume-rendered 3D TEE images or on MPR images ([Figure 13](#)).

In secundum ASD we may distinguish 6 distinct rims listed in a clockwise direction: SVC rim, aortic (anterior) rim, atrioventricular rim, IVC rim, posteroinferior rim, and posterosuperior rim. For the Amplatzer atrial septal occluder, rims capable of securely anchoring the closure device should be



at least 5 mm except for the aortic rim, which should be at least 2 mm. For the Amplatzer multi-fenestrated atrial septal occluder (cribriform device), the SVC and the aortic rim should be at least 9 mm. Absence of the IVC rim is considered a

contraindication for device closure of a secundum ASD. Absence of the aortic rim is a major risk factor for device erosion into surrounding structure, especially when using the Amplatzer atrial septal occluder.

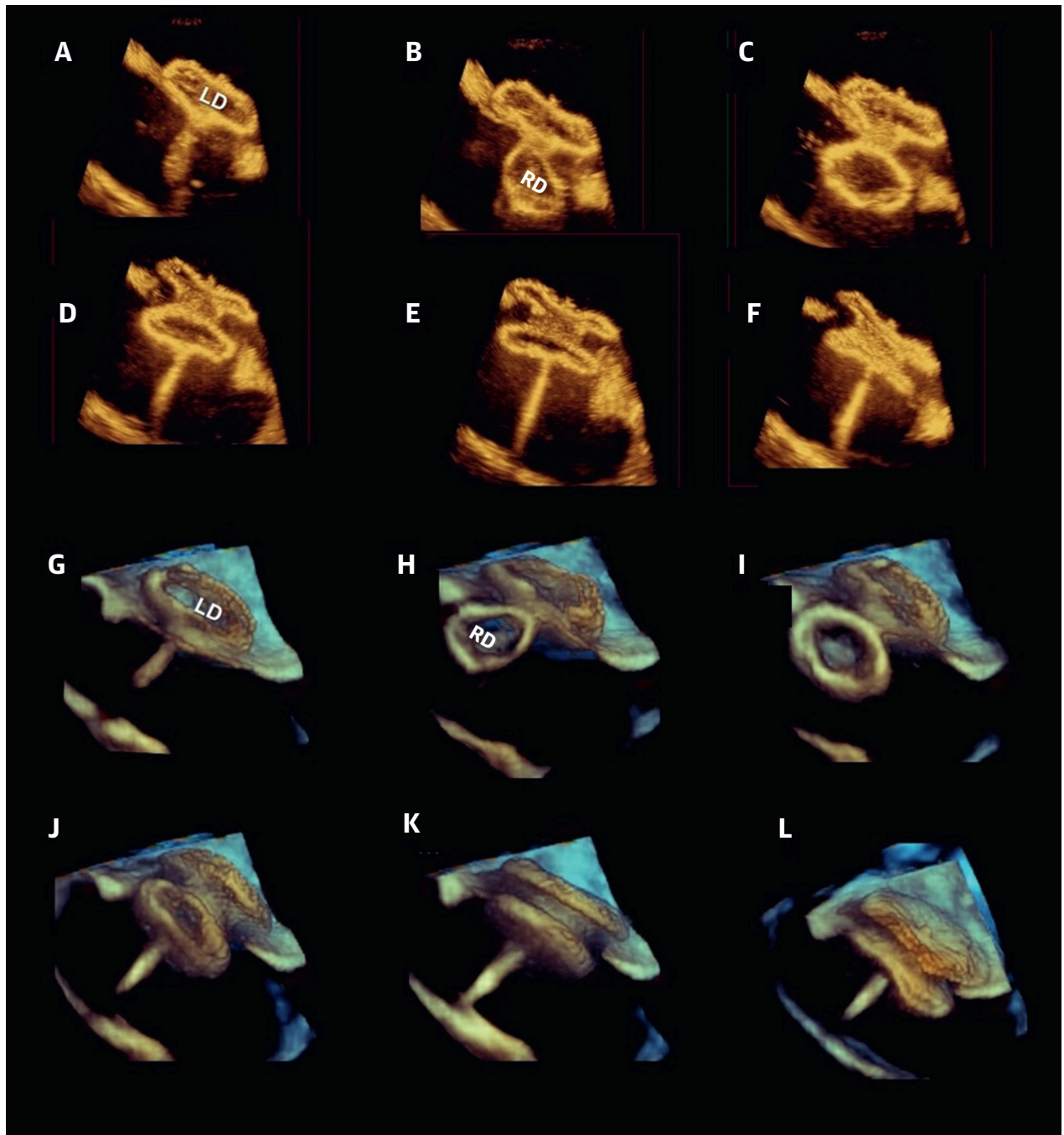
FIGURE 14 Classical 2D/3D TEE Views

(A) 2D TEE mid-esophageal 4-chamber view at 0° with atrioventricular and posterosuperior ASD rims, (B) short-axis at the aortic valve view at 60° with aortic and posteroinferior rims, and (C) bi-caval view at approximately 90° to 120° with SVC and IVC rims. 3D TEE from right (D) and left (E) atrial perspectives. IVC = inferior vena cava; MV = mitral valve; TV = tricuspid valve; other abbreviations as in Figures 2, 3, 8, 10, and 12.

On 2D TEE, ASD should be visualized in at least 3 canonical views: 1) mid-esophageal 4-chamber view at 0° ; 2) short-axis at the aortic valve view approximately at 60° ; and 3) bi-caval view as approximately 90° to 120° . In each view, the maximum ASD diameter during atrial diastole as well as the size of the 2 visible ASD rims should

be measured. At approximately 0° (4-chamber view), atrioventricular and posterosuperior ASD rims are seen. At approximately 60° (short axis view at the level of the aortic valve), aortic and posteroinferior rims are seen. At 90° to 120° (bi-caval view), SVC and IVC rims are visualized (Figures 14A to 14C).

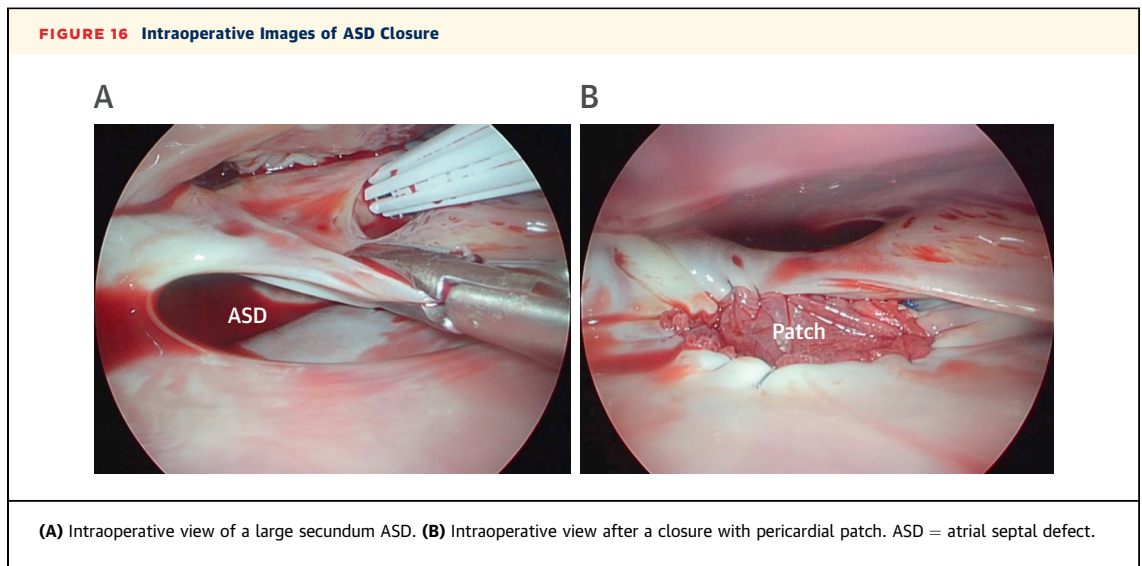
FIGURE 15 Steps of Percutaneous ASD Closure



Steps of percutaneous ASD closure visualized in (A to F) multiplanar reconstruction and (G to L) volume-rendering images. ASD = atrial septal defect; LD = left disc; RD = right disc.

3D TEE imaging is essential for accurate characterization of ASD size, shape, and its rims (Figures 14D and 14E). On 3D zoom en face views the full extent of ASD and its relations to surrounding cardiac

structures can be visualized from both the right atrial and LA perspectives. On 3D TEE imaging, one can establish not only the size but the shape of a secundum ASD (circular, ovoid, or irregular), its location,



and the presence of associated anomalies such as the atrial septal aneurysm.

INTRAPROCEDURAL GUIDE. The most frequently implanted devices consist of a mesh covering opposable double discs (Amplatzer, AGA Medical Corporation, Plymouth, Minnesota), a helix spiral occluder (Helex, W.L. Gore and Associates, Inc., Flagstaff, Arizona), or 2 square umbrella-like spring frames (STARFlex, Inc., NMT Medical, Boston, Massachusetts). The Amplatzer was the first device used. A waist with a thickness of 3 to 4 mm (which roughly corresponds to the thickness of the atrial rims) connects the discs. The size of the device is determined by the diameter of the waist, which may range from 4 to 38 to 40 mm. The 2 discs extend radially, several mm (12 mm) beyond the diameter of the waist, to provide a firm anchorage. The use of 2D/3D TEE requires general anesthesia (although some institutions use TEE under propofol sedation without endotracheal intubation). Classically, the ASD closure requires the defect to be sized using a balloon catheter. The balloon catheter is advanced over the wire under fluoroscopy and TEE control and placed across the defect. The balloon is then inflated until the left-to-right shunt is blocked as observed by 2D TEE color Doppler (balloon stop-flow). The fluoroscopic or echocardiographic indentation of the balloon at the level of the defect margins is the site of measurement. Once the device has been selected, the catheter with the device is advanced in the sheath in the middle of left atrium. The left disk is then expanded and pulled back to the left side of the septum (so that the connecting waist remains across the defect); at this point,

the right disk is expanded in the right atrium, abutting the right side of the septum. After a pull-push maneuver that confirms that it is firmly anchored, the device is released (Figure 15).

POST-PROCEDURAL ASSESSMENT, COMPLICATIONS, AND FOLLOW-UP. Although extremely rare, transcatheter ASD closure is associated with specific complications such as device embolization (0.5% with Amplatzer septal occluder; usually related to wrong size, insufficient rims, or malpositioning), arrhythmias, thrombus formation, erosion, frame fracture, and nickel allergy. Following device closure of an ASD, Doppler imaging should demonstrate either complete or near-complete absence of flow around the device. In contrast, some degree of color Doppler flow through the device is normal and disappears over time as the device endothelializes.

Long-term follow-up of percutaneous ASD closure is typically performed using transthoracic echocardiography to ensure there has been no device migration, erosion into surrounding cardiac structures, or other complications.

SURGICAL CLOSURE

ASD surgery was considered for many years to be the gold standard surgical procedure. Currently the surgical closure remains the therapeutic option for SVC and IVC ASD, ostium primum ASD, unroofed coronary sinus ASD, and secundum ASD only when extremely large (Figure 16). In the vast majority of secundum ASDs, these defects ought to be closed with a patch,

HIGHLIGHTS

- Imaging is of fundamental relevance for LAA and ASD percutaneous and surgical closure.
- Key elements for LAA closure include anatomic characterization, ruling out thrombus, measurements of orifice, and depth.
- Key elements for ASD closure include assessment of type, size, rims, and hemodynamic consequences.

although some small ASDs can be closed with a direct suture. Complications after surgical ASD closure are rare. Typically, atrial arrhythmias occur <15% of the time and, in rare cases, either sinoatrial or atrioventricular node dysfunction requires a pacemaker implantation. Upon successful surgical closure of an ASD, color Doppler imaging should demonstrate complete cessation of prior ASD shunt.

CONCLUSIONS

In this review we provided a detailed description of the anatomy of LAA, of the normal interatrial septum,

and the various types of ASDs as revealed by non-invasive imaging techniques. We described the preprocedure planning and the key steps of the procedural guidance of catheter-based percutaneous closure of LAA and ASD, emphasizing the role of 2D/3D TEE.

AUTHOR DISCLOSURES

Dr. Faletra has performed several talks supported by Philips. Dr. Saric is on the Speakers Bureau of Philips and Medtronic and on Siemens' Advisory Board. Dr. Saw has received unrestricted research grant support from the Canadian Institutes of Health Research, Heart and Stroke Foundation of Canada, National Institutes of Health, University of British Columbia Division of Cardiology, AstraZeneca, Abbott Vascular, Boston Scientific, and Servier; speaker honoraria from AstraZeneca, Abbott Vascular, Boston Scientific, Bayer, and Sunovion; consultancy and Advisory Board honoraria from AstraZeneca, Boston Scientific, and Abbott Vascular; and proctorship honoraria from Abbott Vascular and Boston Scientific. Dr. Hanke has received travel expenses from and is a consultant for Atricure, U.S.A. (receiving <\$10,000 per year). All other authors have reported that they have no relationships relevant to the contents of this paper to disclose.

ADDRESS FOR CORRESPONDENCE: Dr. Francesco F. Faletra, Division of Cardiology, Fondazione Cardiocentro Ticino Via Tesserete 48 CH-6900 Lugano, Switzerland. E-mail: francesco.faletra@cardiocentro.org.

REFERENCES

1. Veinot JP, Harrity PJ, Gentile F, et al. Anatomy of the normal left atrial appendage: a quantitative study of age-related changes in 500 autopsy hearts: implications for echocardiographic examination. *Circulation* 1997;96:3112-5.
2. Di Biase L, Santangeli P, Anselmino M, et al. Does the left atrial appendage morphology correlate with the risk of stroke in patients with atrial fibrillation? Results from a multicenter study. *J Am Coll Cardiol* 2012;60:531-8.
3. Cabrera JA, Ho SY, Climent V, Sanchez-Quintana D. The architecture of the left lateral atrial wall: a particular anatomic region with implications for ablation of atrial fibrillation. *Eur Heart J* 2008;29:356-62.
4. Pritchett EL. Management of atrial fibrillation. *N Engl J Med* 1992;326:1264.
5. Holmes DR, Reddy VY, Turi ZG, et al. Percutaneous closure of the left atrial appendage versus warfarin therapy for prevention of stroke in patients with atrial fibrillation: a randomized non-inferiority trial. PROTECT AF Investigators. *Lancet* 2009;374:534-42.
6. Hanke T. Surgical management of the left atrial appendage: a must or a myth? *Eur J Cardiothorac Surg* 2018;53 Suppl 1:i33-8.
7. Lam YY, Yip GW, Yu CM, et al. Left atrial appendage closure with AMPLATZER cardiac plug for stroke prevention in atrial fibrillation: initial Asia-Pacific experience. *Catheter Cardiovasc Interv* 2012;79:794-800.
8. Cruz-Gonzalez I, Perez-Rivera A, Lopez-Jimenez R, et al. Significance of the learning curve in left atrial appendage occlusion with two different devices. *Catheter Cardiovasc Interv* 2013;83:642-6.
9. Freixa X, Chan J, Tzikas A, Garceau P, Basmadjian A, Ibrahim R. The Amplatzer™ Cardiac Plug 2 for left atrial appendage occlusion: novel features and first-in-man experience. *Euro-Intervention* 2013;8:1094-8.
10. Suwalski P, Witkowska A, Drobiński D, et al. Stand-alone totally thoracoscopic left atrial appendage exclusion using a novel clipping system in patients with high risk of stroke - initial experience and literature review. *Kardiochir Torakochirurgia Pol* 2015;12:298-303.
11. Faletra FF, Nucifora G, Ho SY. Imaging the atrial septum using real-time three-dimensional transesophageal echocardiography: technical tips, normal anatomy and its role in transeptal puncture. *J Am Soc Echocardiogr* 2011;24:593-9.
12. Saric M, Perk G, Purgess J, Kronzon I. Imaging atrial septal defects by real-time 3D transesophageal echocardiography: step-by-step approach. *J Am Soc Echocardiogr* 2010;23:1128-35.
13. Faletra FF, Ramamurthi A, Dequarti MC, Leo LA, Moccetti T, Pandian N. Artifacts in three-dimensional transesophageal echocardiography. *J Am Soc Echocardiogr* 2014;27:453-62.

KEY WORDS atrial septal defect, left atrial appendage, percutaneous closure, surgical closure

APPENDIX For supplemental videos, please see the online version of this paper.